MOLECULAR PHYSICS, 1996, VOL. 89, NO. 4, 1071–1086

Discrete charge effects in the structure of ions around polyelectrolyte models

By J. C. GIL MONTORO and J. L. F. ABASCAL
Departamento de Química-Física, Facultad de Ciencias Químicas, Universidad Complutense de Madrid, E-28040 Madrid, Spain

(*Received 20 February 1996; revised version accepted 11 April 1996*)

Axial long-range effects in the structure of ions around discretely charged polyelectrolytes are discussed. Specifically, we deal with rigid polyion models with helical or cylindrical symmetry—DNA typically—in which a number of charges are treated. The solvent is described by a dielectric continuum. Firstly, exact and approximate methods for calculating the long-range interactions along the axial direction are introduced. The convergence rate and usefulness of the exact formula is discussed. The replacement of the exact expression by that due to an equivalent homogeneous charge distribution is also checked. It is concluded that such substitution leads to erroneous results for the ionic concentration profiles. This seems in contradiction with previous work showing that infinite systems made of discrete and homogeneous charge distributions exhibit very similar ionic structures. Thus, we have investigated the behaviour of the finite systems (i.e. without long-range interactions). It is concluded that polyelectrolyte finite size effects are dependent on the charge distribution: the system with a discrete charge distribution condenses more counterions than the homogeneous one. As the effect of the long-range correction is just the opposite, they mutually cancel so both infinite systems yield almost identical ionic concentration profiles, in agreement with previous studies.

1. Introduction

The increase in computational power of current supercomputers and even desktop workstations makes it possible to examine complex systems and/or properties by computer simulation. This often implies the development of new models describing the interactions between particles in the system. This is needed not only to get more accurate results but also because many properties can only be explained if the model includes the proper features. Polyelectrolyte systems are no exception to this rule and there has been a continuous improvement in their modelling. The very simple homogeneously charged rod-like cylinder was firstly employed [1, 2] to calculate the distribution of counterions using the Poisson–Boltzmann equation. Since then, there has been a number of computer simulations on this system [3–9]. Many of the polyelectrolyte properties—those depending essentially on the mean electric field—are described by the hard charged cylinder model. It has been shown that several other experimental results are better predicted theoretically by assuming that the repulsion of the polyion core is soft. An example of this is the energy transfer between the solution ions in the presence of DNA [10]. For many properties, however, the simulations using a soft repulsive polyion [11–13] do not show a qualitatively different behaviour to that of the hard system, sometimes its use being a question of computational convenience (for instance in molecular dynamics simulations).

The existence of several packages enabling the simulation of full atom models has opened a wide gap in the modelling of these systems. Very often, the information obtained with such packages is too detailed and difficult to interpret. Although such models are required for specific phenomena—e.g. interpretation of NMR experiments—there is a clear need for models with an intermediate level of detail but capable of accurately predicting as much as the real system's properties as possible. For instance, the counterion concentration profile observed in full atom DNA simulations [14] shows a double hump instead of the sharp peak usually obtained when simpler models are used. This need might be fulfilled by a variety of simple models in which a discrete representation is used for the polyion charge [8, 15–18]. These kinds of models often place unit negative charges at the phosphate positions. The work done on simple helical models has, however, been rather discouraging. A slight increase in the counterion condensation was the only difference observed from the behaviour of homogeneously charged polyions. Nevertheless, in a recent paper [13] we have shown that when a helical model is supplemented with an appropriate treatment of the excluded volume (the repulsive interactions modelling the DNA grooved shape in a very simple manner) many features typical of full atom models, in particular the double hump in the counterion concentration profile, are also described. It seems then that the behaviour of a simple DNA model but with some explicit treatment of the charges (what we call discretely charged models) deserves some attention.

The simulation of systems with coulombic forces poses a number of problems. Because of their long range, electrostatic interactions require the calculation of the potential created by a great number of simulation box replicas. When the polyion has (roughly) cylindrical symmetry, the inhomogeneity of the system suggests a different treatment for the long-range potential along the axial and radial directions. The latter is frequently avoided by using a finite cell, i.e. a hard repulsive container which limits the radial direction, though such a discontinuous boundary may lead to some undesired effects. An alternative is to allow a transition region in which the coulombic interactions are modulated and progressively transformed into short range forces [19]. Beyond the transition region, all the charged particles are treated as short-ranged which leads to a bulk region with boundary conditions similar to those of simple fluids, hence the method name modulated bulk as a fuzzy boundary (MBFB).

The corrections due to the long-range forces along the axial directions are even more necessary. This is due to the fact that the anisotropic charge distribution is repeated *ad infinitum* in those directions [19]. In the extended image method, the infinite polyion and its surrounding counterions are replaced by a basic cell and one or more replicas above and below it [8, 20, 21]. The procedure of Torrie and Valleau [22] is clearly a better choice as it considers as infinite polyelectrolyte. There, the effect of the ionic charge distribution outside the simulation box is included as a mean-field term computed self-consistently from the average charge distribution within the cell. For the long range interaction with the polyelectrolyte, the situation is not so clear. The electrostatic potential between an infinite polyion and a solution ion is well known in the case of a homogeneously charged body like a line of charge or a charged cylinder [4]. But when the macromolecule consists of discrete charges the latter formula is no longer valid. In this work we check an exact expansion to sum the contributions when the charges are placed as arrays of points along several lines parallel to the axial direction, which is typically the case in simple helical DNA models. The expression has been known for some time but, to our knowledge, it has not been used in computer simulations until now [13]. The relation is first examined to study its limiting and

convergence properties and then used to investigate the effect of the charge discretization.

A second issue is to assess to what extent the exact formula can be replaced at large distances by that corresponding to a line of charge with the same charge density. It will be shown that such a substitution has a significant effect on the ionic concentration profiles. This seems to contradict previous work showing that—provided that no special excluded volume effects are present—discretely and homogeneously charged polyelectrolytes with the same charge density behave similarly. It is difficult to explain from this how the inclusion of exact expressions for the long-range potential could modify the situation. In order to solve the apparent contradiction we report the results for simulations *excluding* the axial long-range interaction. We will show that, in such a case, discrete and homogeneously charged models behave distinctly, the departures between them being opposite to those produced by the corresponding long-range corrections. The cancellation of these opposing effects makes it possible that homogeneous and discrete models show similar ionic profiles and enables the interpretation of apparently contradictory results.

In summary, the objective of this work is twofold. Firstly, to discuss the effect of using exact and approximate formulas for the long-range potential along the axial direction in the simulation of discretely charged polyelectrolyte models. The second, and perhaps more important, the goal of the paper is to show that the study of the long-range interactions allows a better understanding of the effects induced on homogeneous polyelectrolytes by the discretization of their charges.

2. Polyelectrolyte models and potential interactions

In this section we describe the interactions for the system within the basic simulation cell. Two polyelectrolyte models—roughly representative of B-DNA in solution—are compared in this work. Our simplest model is a homogeneously charged soft (HS) cylinder (denoted as HS1 in [13]). From the electrostatic point of view it is equivalent to a line of charge at the DNA axis but it is supplemented with a repulsive potential to account for the DNA volume. The Coulombic interaction between an ion and the finite segment of the line of charge within the simulation box (of height L) is [4]

$$U_{ip}^{\text{line, }L}(\rho_{ip}) = -2z_i\xi\beta^{-1}\sinh^{-1}\left(\frac{L}{2\rho_{ip}}\right), \tag{1}$$

where the subscript ip denotes a variable dependent on ion–polyion distances. Accordingly, ρ_{ip} is the radial coordinate (distance to the polyion axis) of ion i. z_i is the ionic valency and ξ the reduced axial charge density of the polyion

$$\xi = \lambda_B/b, \tag{2}$$

b being the distance between charges along the polyelectrolyte axis (b = 1·69 Å for B-DNA) and λ_B the Bjerrum length. This is defined as

$$\lambda_B = \frac{e^2\beta}{4\pi\varepsilon_0\varepsilon}, \tag{3}$$

where e is the magnitude of the electronic charge, $\beta = 1/(k_B T)$—k_B being the

Boltzmann constant and T the temperature—ε_0 is the vacuum permittivity and ε the (relative) dielectric constant of the solvent. For water at 25 °C, ε = 78·358 so that λ_B = 7·15 Å, giving ξ = 4·23.

A refinement of the previous model is the substitution of the homogeneous charge by a (fixed) set of discrete charges. Most of the DNA charge lies at the phosphate groups [23]. Thus, in the discrete model discussed here, the charges are set with helical symmetry at the positions of the phosphorus atoms whose cylindrical coordinates for canonical B-DNA are [24]

$$\left.\begin{aligned} \rho_i^s &= 8{\cdot}91 \\ \phi_i^s &= \phi_0^s + 36\, i \\ z_i^s &= z_0^s + 3{\cdot}38\, i, \end{aligned}\right\} \tag{4}$$

where s = 1, 2 specifies the nucleic acid strand, and i = 0, ..., 9, describing a full DNA helix turn. The distance parameters ρ and z are given in angstrom and ϕ in degrees. Besides, ϕ_0^s and z_0^s are both zero for the phosphates in the first strand, and 154·4° and 0·78 Å, respectively, for those in the second. The 3·38 Å rise and the 36° rotation per residue lead to the well-known fact that B-DNA has 10 base pairs per helix turn with a 33·8 Å pitch. We refer to this model as DS (discretely charged, soft repulsive potential). The potential between the charged DNA sites within the simulation box (of height L) and a solution ion is simply

$$U_{ip}^{\text{helix},L} = \sum_{\alpha} U_{i\alpha}^{\text{cou}}(r_{i\alpha}), \tag{5}$$

where the sum extends over DNA sites α, $r_{i\alpha}$ is the distance between site α and ion i and $U_{i\alpha}^{\text{cou}}$ is the coulombic potential which is obviously the same irrespective of whether the charges are either fixed or mobile. Thus, in general

$$U_{ij}^{\text{cou}}(r_{ij}) = \frac{z_i z_j}{4\pi\varepsilon_0\varepsilon}\frac{e^2}{r_{ij}}. \tag{6}$$

The short-range repulsive interactions with DNA are described in both models by means of a soft potential of the form [13]

$$U_{ip}^{\text{rep,poly}}(\rho_{ip}) = K_{ip}\frac{1}{(\rho_{ip}-\rho_0)^n}. \tag{7}$$

For n = 9, K_{ip} = 2·7291 × 10^{-17} J Å^9, and ρ_0 = 8·91 Å; the maximum in the radial distribution of counterions appears at about 12 Å [13]. The mobile ions are considered to be soft as well,

$$U_{ij}^{\text{rep,ions}}(r_{ij}) = K_{ij}\frac{1}{r_{ij}^n}, \tag{8a}$$

$$K_{ij} = \frac{A_M|z_i z_j|e^2}{4\pi\varepsilon_0 n N_c}(r_i + r_j)^{(n-1)}, \tag{8b}$$

r_{ij} being the distance between ions i and j. The choice of A_M = 1·7476 (the Madelung constant of the NaCl solid structure), and N_c = 6 (the coordination number of the same structure) together with the value r_i = 1·4214 Å (the nominal radius of ion i) taken for both anions and cations, gives bulk electrolyte properties approximately

corresponding to a restricted primitive model with hard-sphere diameters of 4·2 Å [25]. This size has been widely used in recent electrolyte and polyelectrolyte solution studies [13, 26–33] and roughly corresponds to a sodium ion with its hydration shell [28, 29].

3. Long range interactions with the polyelectrolyte

3.1. *A single array of charges*

The interaction of a charge with an infinitely long array of charges spaced out (embedded in a straight line) is

$$U^{\text{array,inf}}(\rho, \Delta z) = 2z_i\xi_v\beta^{-1}\left[\log\rho - 2\sum_{j=1}^{\infty} K_0(\kappa_j\rho)\cos(2\pi j\,\Delta z/d)\right] \tag{9}$$

where ρ is the distance from the ion to the array, z_i the valency of the charge, ξ_v the reduced axial charge density of the array, Δz the axial coordinate of the ion with respect to the closest charged site, d the distance between two consecutive charges along the array, and K_0 is the modified Bessel function of order zero and of the second kind. The first term is the potential of an infinite homogeneous line of charge (see the Appendix)

$$U^{\text{line,inf}}(\rho) = 2z_i\xi\beta^{-1}\log\rho \tag{10}$$

and the second is the discrete charge contribution. The above equation has been known for some time, and was rederived by Soumpasis [34] in the context of theoretical work on model polyelectrolytes but, as far as we are aware, has not yet been used in computer simulations. The summation on the right hand side of equation (9) is quickly convergent so few terms are needed. This can be seen in figure 1 where we plot the number of terms required to reach an accuracy of 0·001%. The convergence is quite dependent on the radial separation from the array but almost independent on the axial coordinate. The summation is not required at all—i.e. the line of charge and the array yield the same potential—at radial distances comparable with the separation of charges in the array and beyond; fewer than 10 terms are required for most of the remaining distances.

In the limit $\rho \to 0$, both the absolute value of the logarithm and the series term in equation (9) tend to infinity despite the fact that the potential asymptotically approaches a limiting value (see figure 2). The evaluation of the long-range interaction in these circumstances is somewhat ill-conditioned and requires many terms. A specific exact summation is preferable in such a case as it provides a simple and compact expression (see the Appendix for the derivation). It reads

$$\lim_{\rho\to 0} U^{\text{array,inf}}(\rho, \Delta z) = z_i\xi_v\beta^{-1}\left[\psi\left(\frac{\Delta z}{d}\right) + \psi\left(1-\frac{\Delta z}{d}\right) + 2\log(2d)\right], \tag{11}$$

where $\psi(x)$ is the so-called digamma (or *psi*) function [35].

In figure 2 we show the potential $U^{\text{array,inf}}$ as a function of ρ for several $\Delta z/d$ values. The behaviour at large ρ is independent of $\Delta z/d$; indeed, as observed in figure 1, the effect of the discretization of the charge vanishes at distances comparable with the separation between the charges in the array. At smaller radial distances, the curves deviate from that of the line of charge, the slope of the curves increasing with $\Delta z/d$. Finally, at very low ρ, $U^{\text{array,inf}}$ is essentially equal to the value at $\rho = 0$. This is an interesting result as it shows that equation (9) does not need to be used in the region

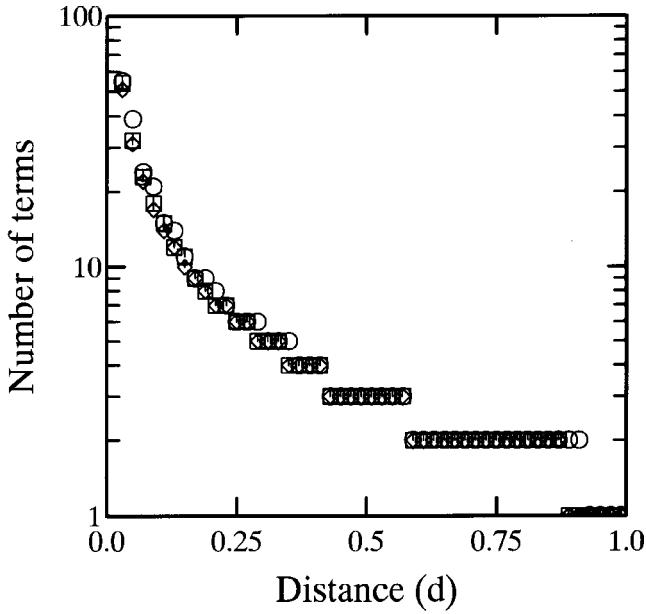

Figure 1. Number of terms required to achieve an accuracy of 0·001% in equation (9) as a function of the distance to the array of charges ρ (in d units, d being the separation between charges along the array). $\Delta z/d = 0$, boxes; 0·16, diamonds; and 0·5, circles. Notice the logarithmic scale of the y-axis.

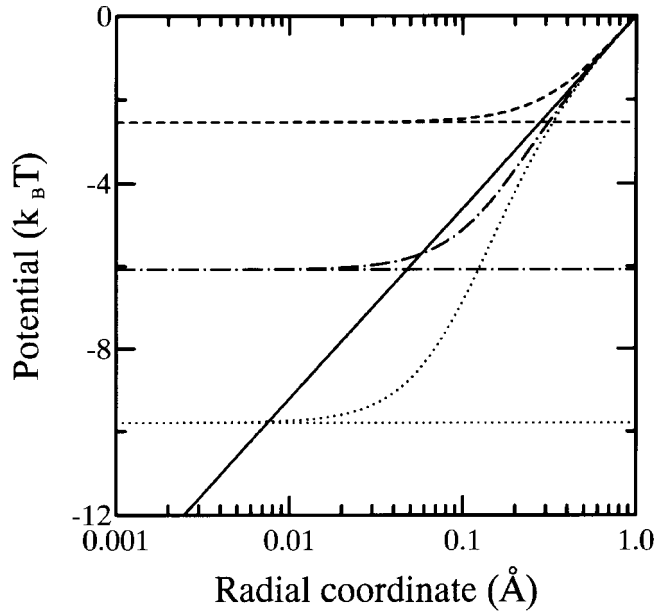

Figure 2. Electrostatic potential between an array and a monovalent mobile ion for different $\Delta z/d$ values: 0·5, dashed curve, 0·16, dash-dotted; and 0·1, dotted. The full curve is the potential for a line of charge with the same charge density. Notice the logarithmic scale of the x-axis.

in which it is badly conditioned. In particular, in the case of the arrays which build-up our helical BDNA model, the formulas appropriate for computation are

$$U^{\text{array,inf}} = \begin{cases} \text{Equation (11)}, & \text{for} \quad \rho < 0{\cdot}01d \\ \text{Equation (9)}, & \text{for} \quad 0{\cdot}01d < \rho < d \\ \text{Equation (10)}, & \text{for} \quad d < \rho. \end{cases} \tag{12}$$

3.2. *Exact formulas for the simple B-DNA helical model*

B-DNA has 10 phosphorus atoms per helix turn in each of the strands, and, thus, there are 20 charged sites per turn in the case of our helical models. As each of the charged sites generates an array of charges when the basic cell is infinitely replicated along the axial direction, the total potential between the charges in an infinite DNA helix and a solution ion is

$$U_{ip}^{\text{helix,inf}} = \sum_{\nu} U^{\text{array,inf}}(\rho_{\nu}, \Delta z_{\nu}), \tag{13}$$

where the subscript ν refers to any of the 20 arrays of charge and thus $\xi_{\nu} = \xi/20$.

We are interested in separating the contributions coming from the particles within the simulation cell from those outside it. Such a separation seems nonsensical in our systems since exact formulas exist both for the homogeneously charged cylinder and the helical model. Nevertheless, it is necessary for the purposes of this paper. The homogeneous long-range potential, i.e. the potential due to a homogeneous charge distribution outside the simulation box, U_{lr}^{line}, is the difference

$$U_{lr}^{\text{line}}(\rho_{ip}) = U^{\text{line,inf}}(\rho_{ip}) - U^{\text{line,}l}(\rho_{ip}), \tag{14}$$

with $U^{\text{line,inf}}(\rho_{ip})$ and $U^{\text{line,}l}(\rho_{ip})$ given by equation (10) and (1), respectively. Analogously, the long-range interaction in the helical model, U_{lr}^{helix} may be defined as the departure of $U^{\text{helix,inf}}$ from the sum of the coulombic interactions of the mobile ion with each of the polyion charges inside the box

$$U_{lr}^{\text{helix}} = U_{ip}^{\text{helix,inf}} - U_{ip}^{\text{helix,}l}. \tag{15}$$

3.3. *The homogeneous approximation*

No previous simulations of discretely charged models (apart from those reported in [13]) have used the exact equation for the axial long-range correction. Indeed, equation (14) was so well established in homogeneously charged polyelectrolyte systems that its use seemed also natural in helical DNA models [7, 16]. We will refer to the replacement, in discretely charged models, of the exact axial long range interaction, U_{lr}^{helix}, by that of a homogeneous line of charge, U_{lr}^{line}, as the homogeneous (long-range) approximation (HA). The validity of such a replacement depends on whether the relation

$$U_{lr}^{\text{helix}} \simeq U_{lr}^{\text{line}} \tag{16}$$

is accurate enough. The conclusions obtained for the array of charge when $\rho > d$ could also be taken as supporting the HA approximation. However, it is important to stress that the behaviour of the array of charge is close to that of the uniformly charged line at radial ion–polyelectrolyte distances which are short *relative to the separation*

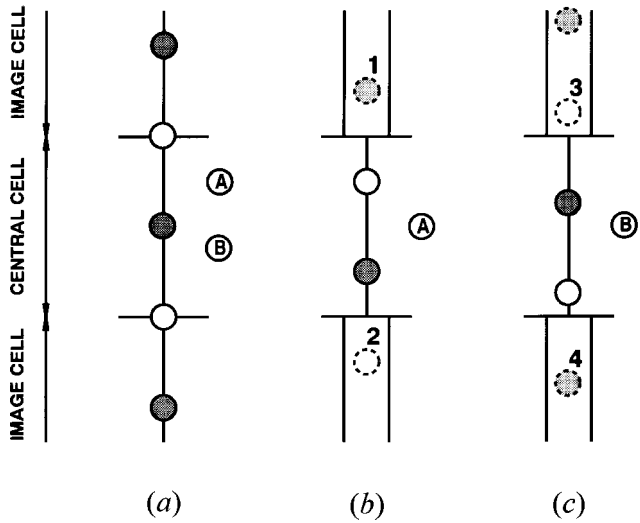

Figure 3. (*a*) Scheme of a discrete polyelectrolyte with two mobile ions and the use of periodic boundary conditions in the axial direction. (*b*) the system as seen by ion A with the homogeneous long-range approximation and (*c*) as seen by ion B.

between the charges in the array. The separation in our B-DNA model is just the helix pitch which is about 30 Å. On the other hand, even if the *full* replacement of one or all of the arrays were justified, until now no argument has been given which enables the substitution of a *part of the system* along the *axial* direction. This is better understood with the aid of the scheme of figure 3. For simplicity, let us consider here a polyelectrolyte with two charges (one hollow and one shaded) placed along the axis. In part (*a*) of the figure we plot the central simulation cell. Part of the upper and lower image cells are also included as well as two mobile ions labelled A and B. In (*b*) and (*c*) we represent the system as seen by ions A and B, respectively, when the HA approximation is put into effect. By virtue of the periodic boundary conditions, the explicit part of the polyelectrolyte acting on each ion is centred on it. From a distance equal to half the height of the simulation cell the charges are homogenized. The closest polyelectrolyte sites not explicitly considered are sites 1 and 2 for ion A, and sites 3 and 4 for ion B. The approximation does not affect both ions equally: site 3 is closer to ion B than sites 1 and 2 are to ion A, but the long-range correction along the axial direction is the same for ions A and B in the HA approximation.

Figure 4 shows the error (in $k_B T$ units) of the HA approximation, $U_{lr}^{\text{helix}} - U_{lr}^{\text{line}}$, as the ion approaches the helical DNA model from several positions. Each curve represents the values obtained when the orientation relative to the axis is kept constant—see the chosen orientations in figure 5—and the radial coordinate ρ varies. For this figure, the simulation box included two helix turns along the axial direction (explicitly). The error changes from one orientation to another though not drastically and is not negligible even at large distances. Figure 6 gives the actual values (in $k_B T$ units) of the error in the potential energy for three different cell heights (those including 1, 2, and 3 complete DNA turns, respectively) for the case of an ion approaching DNA along the phosphate positions. The error is significant up to about 40 Å. Beyond that distance it is almost independent of the cell size. By contrast, in the region close to the polyelectrolyte, the error is strongly dependent on the box height diminishing with bigger simulation boxes as expected.

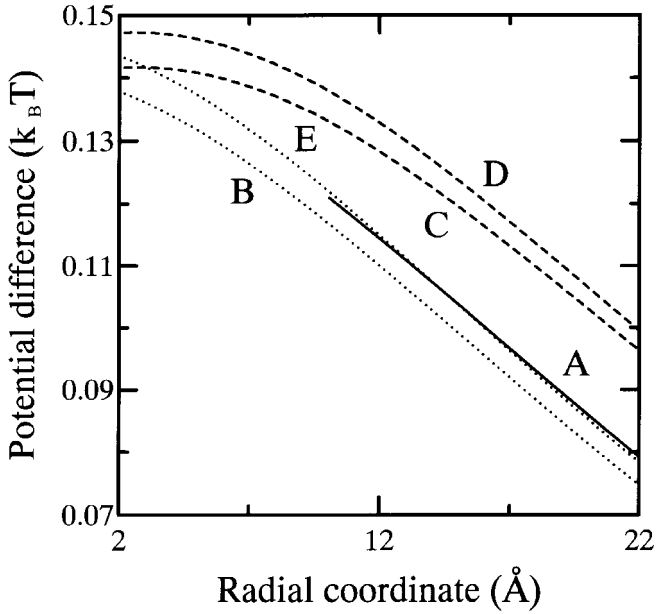

Figure 4. Difference of the long-range polyelectrolyte potential of the discrete model with respect to that of an equivalent homogeneous model (i.e. the error of the HA approximation), $U_{Ir}^{\text{helix}} - U_{Ir}^{\text{line}}$, for an ion approaching DNA from different angular and axial coordinates. The axial cell size includes two DNA turns. A, in front of a phosphate; B, in the middle of the minor groove, at the same height as a phosphate; C, in the middle of the major groove, at the same height as a phosphate; D, in the middle of the major groove, at a height between two phosphates; and, *E*, in the middle of the minor groove, at a height between two phosphates (see figure 5).

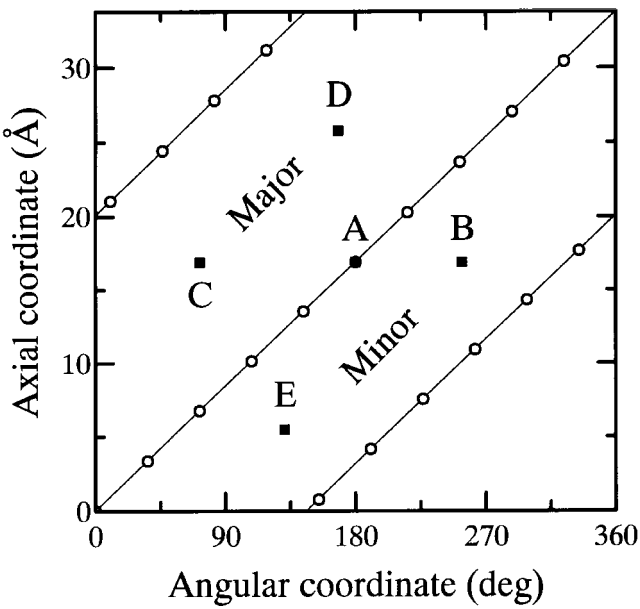

Figure 5. Projection of the cylinder containing the charged sites onto a plane. The solid boxes give the orientations relative to DNA of the points used in figure 4 and open circles represent the positions of the charges.

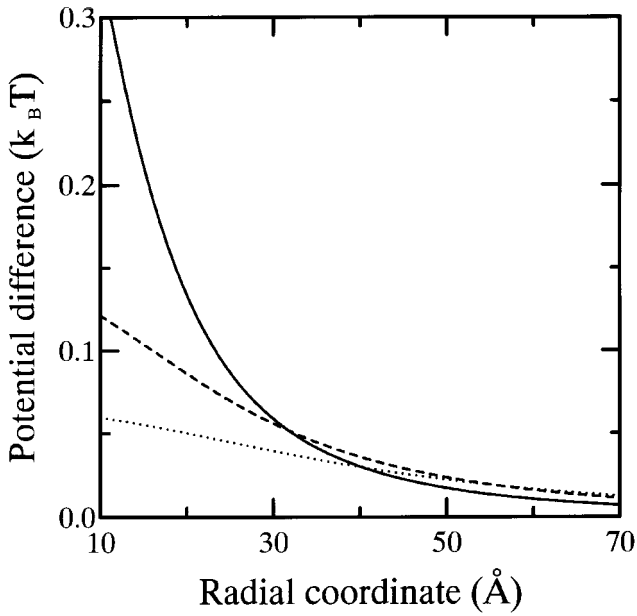

Figure 6. Error of the HA approximation, $U_{lr}^{\text{helix}} - U_{lr}^{\text{line}}$, for an ion approaching DNA in front of a phosphate (point A in figure 5) when using different axial cell sizes measured in DNA helix turns. Solid curve, one turn; dashed, two turns; and dotted, three turns.

4. Effect on the ionic concentration profiles

Until now we have calculated the long-range potential due exclusively to the polyelectrolyte charges outside the cell. But the calculation of the long-range interaction also involves the effect of the external solution ions. As these ions are mobile, the contribution changes from one configuration to another. It is accepted that its effect may be included as a mean field from the average charge distribution within the cell [22]. The appropriate expression is

$$\left.\begin{aligned} U_{lr}^{\text{ions}}(\rho_{ip}) &= 2 z_i \lambda_B \beta^{-1} \int_0^R B(\rho_{ip}, r') \left[\sum_i z_i C_i(r') \right] r' \mathrm{d}r' + U^* \\ B(\rho_{ip}, r') &= -\int_0^{2\pi} \ln\left(\frac{L}{2} + \left(\left(\frac{L}{2} \right)^2 + \rho_{ip}^2 + r'^2 - 2\rho_{ip} r' \cos\phi \right)^{1/2} \right) \mathrm{d}\phi, \end{aligned} \right\} \tag{17}$$

where R is the radius of the cell, and the sum on the RHS represents the total radial charge density at a distance r' from the polyion (the sum extends over all charged species and $C_i(r')$ is the radial concentration profile of species i). The ionic concentration profiles are dependent on the thermodynamic state—unlike previous calculations—so the evaluation of the above expression requires a complete simulation of that particular state. We have carried out simulations for the discrete and the homogeneously charged models with their corresponding long-range interactions and also for the DS model using the homogeneous approximation. For other technical details of the simulations see [13]. Once the radial density profiles are available from the simulations, it is possible to evaluate the long-range potential due to the ions outside the cell. Of course, this must be done self-consistently within the simulations as the inclusion of the long-range interactions modifies the concentration profiles from

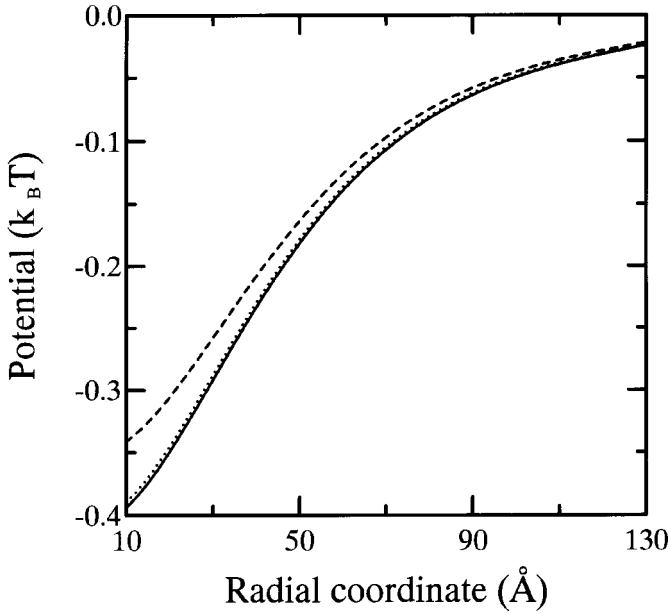

Figure 7. Magnitude of the total long-range axial potential (due to the polyelectrolyte and the mobile ions outside the cell) for an ion approaching a phosphate. The monovalent salt concentration is 0·05 M in all cases and the simulation box explicitly includes three DNA turns. Solid curve, HS system; dashed, DS; and dotted, DS+HA (i.e. using the homogeneous approximation instead of the exact long-range interaction for the DS model).

those obtained without such a correction. In figure 7 we plot the total long-range correction (due to the polyelectrolyte and to the mobile ions) for the HS and DS systems using the proper treatment, and for the DS model using the HA approximation, all of them at 0·05 M monovalent salt concentration. It can be seen that the HA approximation yields a long-range interaction, quite similar to the 'exact' values for the HS model which, in turn, differ from those for the discretely charged system.

Despite all the previous calculations, we have no clear evidence of how much the approximation affects the system behaviour. Perhaps the most representative microscopic properties of these polyelectrolyte solutions are the ionic concentration profiles. The profiles obtained in a simulation are rather noisy and the departures between the different systems appear as small drifts superimposed on the noise. In these circumstances the comparisons are quite difficult. There is a related function which is better conditioned for the small but systematic differences between the models. It is the charge compensation function, $Q(\rho)$, which describes the way in which the mobile ions gradually cancel the polyion charge. It is defined as

$$Q(\rho) = \sum_i q_i(\rho), \tag{18a}$$

$$q_i(\rho) = 2\pi z_i b \int_0^{\rho} C_i(\rho')\,\rho'\,\mathrm{d}\rho', \tag{18b}$$

where the sum extends over ionic species. $Q(\rho)$ is zero at $\rho = 0$ and increases with distance reaching unity in the bulk.

In figure 8 we represent the charge compensation functions both with and without

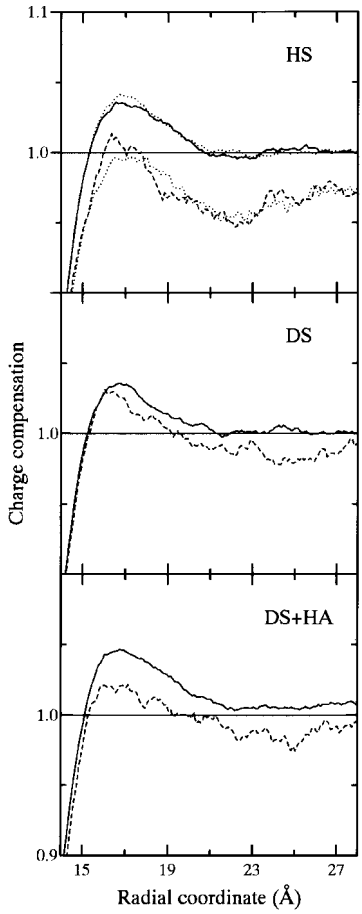

Figure 8. Charge compensation functions for the models considered at 2·5 M monovalent salt concentration. The basic cell includes two DNA turns. Solid curves, infinite polyelectrolyte systems including long range axial interactions; dashed, same systems without long range axial corrections. In general, the curves are obtained using a hard-cell boundary along the radial direction, the exception being the dotted curves of the upper graph where simulations have been performed with a radial fuzzy boundary (the MBFB method described in [19]).

the long-range potentials. Notice that the system being simulated in the absence of axial long-range interactions is actually a finite polyelectrolyte, i.e. an 'oligoelectrolyte' in which end-effects are missing due to the periodic boundary conditions. In the simulations, two different treatments of the long-range forces along the radial direction have been used, namely, a hard cell and a fuzzy boundary (the MBFB method described in [19]). The upper curve shows that, at least for the HS model, a finite cell boundary leads to charge compensation functions similar to those given by the MBFB method although the concentration profiles of the cell boundary are severely distorted in the region close to the hard wall at this high salt concentration [19]. The same has been observed in other systems not depicted in the figure. It is concluded that the departures between the different systems are exclusively due to differences in the charge distributions and to the treatment of the long-range interactions along the axial direction.

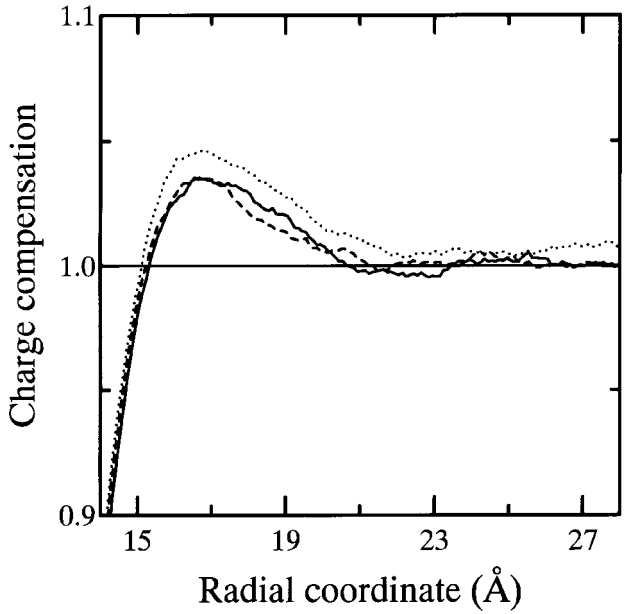

Figure 9. Charge compensation functions for the infinite systems (i.e. including long range interactions). Solid curve, HS system; dashed, DS; and dotted, DS+HA.

Finite size effects are quite marked even though end-effects are missing in our finite polyelectrolytes. In general, the long-range interactions tend to condense the counterions more closely to the polyion [11]. Thus, the curves for the finite systems reach their asymptotic values at larger distances. The long-range correction does not affect the homogeneous and discrete charge distribution models in the same way. It can be seen in figure 8 that the charge compensation functions for the HS and DS models are considerably different when the long-range potentials are not accounted for. In such a case the HS system condenses fewer counterions in the vicinity of the DNA molecule than the DS model. Nevertheless, its corresponding long-range correction is much more important. Interestingly, the resulting charge compensation functions for the infinite polyelectrolytes are quite similar for both models which is in agreement with previous observations [13]. The conclusion that the ionic concentration profiles are essentially the same for systems with identical charge density independently of the polyion charge distribution could represent the general behaviour of infinite systems. This is because the stronger the condensation of counterions around a given finite charge distribution, the higher the screening they produce and, thus, the smaller the magnitude of the long-range interactions. A smaller number of counterions condensed by the effect of the long-range corrections is a consequence of the stronger condensation produced by a finite discretely charged system. Just the opposite holds for a homogeneous charge distribution.

From these premises, it is easy to understand that the HA approximation is inconsistent since it incorporates the (strong) long-range correction due to the homogeneous polyelectrolyte charge to a finite system made of discrete charges (whose counterion condensation is also strong). In this way, the long-range potential 'over corrects' (see figure 8) and the HA approximation yields an overcondensation of counterions even at large distances. In figure 9 we depict the charge compensation

function of the three (infinite) polyelectrolyte systems, HS, DS, and DS+HA. The plot shows even more clearly that the homogeneous and the helical systems behave in a very similar way and confirms that the use of the HA approximation instead of the correct expression in discretely charged models yields incorrect results.

5. Conclusions and discussion

In this paper we have shown that appropriate formulas for the calculation of long-range interactions along the axial direction in discretely charged polyelectrolyte models are manageable. Its limiting expression at very small distances avoids the appearance of ill-conditioned calculations. But the interest of the paper goes beyond this, as our study has allowed a better characterization of the behaviour of these systems. The similarities in the ionic concentration profiles and charge compensation functions of homogeneously and discretely charged polyelectrolytes with identical charge density have been justified as the result of two mutually cancelling effects. A 'finite' polyelectrolyte with a discrete charge distribution condenses more ions than the equivalent homogeneously charged system but the opposite holds for their long-range contributions. Besides, it has been proven that the use of a homogeneous approximation is inconsistent in discretely charged models. Notice that the concentration profiles are cylindrically averaged properties. This is consistent with the potential model in the case of the homogeneous charge distribution but not in the discrete case. In a forthcoming paper we will show deviations from cylindrical symmetry. As expected, the counterions condense close to the positions of the charges in the helical model. Since the repulsive forces of the polyelectrolyte models used in this work prevent the counterions from entering into the DNA grooves, the possible effect of the entrant counterions is neglected. The same does not hold when the potential model incorporates the grooved DNA structure. For such a model, the departures of the cylindrically averaged concentration profiles from the homogeneous one are noticeable although they vanish a few angstroms beyond the phosphate positions [13]. As a final conclusion, let us note that the last figures of this work confirm that finite size effects are important in these systems [11] despite the fact that periodic boundary conditions are applied, and, thus, end-effects cannot appear.

This work was partially supported by Grant PB93-0085 from the Dirección General de Investigación Científica y Tecnológica of Spain. J. C. Gil Montoro acknowledges a FPI grant from the Spanish Ministry of Education.

Appendix

Consider an infinite array of point charges of (negative) valence z_p placed along a line at equally spaced intervals of length d. The electrostatic energy of an ion of valence z_i located a distance from the array is given by equation (9). This appendix addresses the limit of such an electrostatic interaction when the ion is placed precisely in the line passing through the array charges, a situation for which equation (9) diverges. It is convenient to start with the potential created by an infinite continuous line of charge. The electrostatic energy of the ion at a distance ρ to the middle of the segment is [4]

$$U^{\text{line},L}(\rho) = -2z_i\xi\beta^{-1}\sinh^{-1}\left(\frac{L}{2\rho}\right). \tag{A 1}$$

The infinite line case is then

$$U^{\text{line,inf}}(\rho) = \lim_{L\to\infty} U^{\text{line},L}(\rho) = \lim_{L\to\infty} 2z_i\xi\beta^{-1}\log\left(\frac{\rho}{L}\right), \tag{A 2}$$

or

$$U^{\text{line,inf}}(\rho) = 2z_i\xi\beta^{-1}\log\rho - U^*, \tag{A 3}$$

with

$$U^* = \lim_{L\to\infty} 2z_i\xi\beta^{-1}\log L. \tag{A 4}$$

The diverging term U^* of equation (A 3) is a consequence of the infinite charge of the line, and is not usually included as it cancels out an equal contribution, but of opposite sign, from the mobile ion profiles equation (17). The potential created by an array of discrete charges, equation (9), also lacks a $-U^*$ term.

We go back to the problem motivating this Appendix. The probe ion is at distances Δz and $d-\Delta z$ from the two closest array charges, one above and the other below it. Successive array charges are found at distances $d, 2d, \ldots$ from these two in each direction. The coulombic energy of the ion is then

$$U^{\text{array,inf},0} = z_i\lambda_B\beta^{-1}\lim_{n\to\infty}\sum_{j=0}^{n}\left(\frac{z_p}{\Delta z+jd}+\frac{z_p}{d-\Delta z+jd}\right). \tag{A 5}$$

Applying the recurrence formula of the psi function $\psi(x) = \mathrm{d}[\log\Gamma(x)]/\mathrm{d}x$ n times [35],

$$\psi(x+1) = \psi(x)+\frac{1}{x} \tag{A 6}$$

yields

$$\psi(x+n+1) = \psi(x)+\sum_{i=0}^{n}\frac{1}{i+x}, \tag{A 7}$$

which after calculating the limit as n goes to infinity and using the known asymptotic behaviour of the psi function ($\psi(x) \sim \log x$ as $x\to\infty$) allows us to write

$$\lim_{n\to\infty}\sum_{i=0}^{n}\frac{1}{i+x} = \lim_{n\to\infty}\log n - \psi(x). \tag{A 8}$$

With the aid of equation (A 8) and introducing the reduced axial charge density of the line $\xi = -\lambda_B z_p/d$, equation (A 5) transforms into

$$U^{\text{array,inf},0} = z_i\xi\beta^{-1}\left[\psi\left(\frac{\Delta z}{d}\right)+\psi\left(1-\frac{\Delta z}{d}\right)-2\lim_{n\to\infty}\log n\right]. \tag{A 9}$$

For a given n, the length of the array is $L = 2nd$ so that

$$U^{\text{array,inf},0} = z_i\xi\beta^{-1}\left[\psi\left(\frac{\Delta z}{d}\right)+\psi\left(1-\frac{\Delta z}{d}\right)+2\log(2d)\right]-2z_i\xi\beta^{-1}\lim_{L\to\infty}\log L, \tag{A 10}$$

or

$$U^{\text{array,inf},0} = z_i\xi\beta^{-1}\left[\psi\left(\frac{\Delta z}{d}\right)+\psi\left(1-\frac{\Delta z}{d}\right)+2\log(2d)\right]-U^*, \tag{A 11}$$

where the diverging term again appears in a natural way.

References

[1] Fuoss, R. M., Katchalsky, A., and Lifson, S., 1951, *Proc. Natl. Acad. Sci. USA*, **37**, 579.
[2] Alfrey Jr, T., Berg, P. W., and Morawetz, H., 1951, *J. Polymer Sci.*, **7**, 543.
[3] (a) Bratko, D., and Vlachy, V., 1982, *Chem. Phys. Lett.*, **90**, 434; (b) J. Reščič, and Vlachy, V., 1994, *ACS Symp. Ser.*, **548**, 24.
[4] Mills, P., Anderson, C. F., and Record Jr, M. T., 1985, *J. phys. Chem.*, **89**, 3984.
[5] Olmsted, M. O., Anderson, C. F., and Record Jr, M. T., 1991, *Biopolymers*, **31**, 1593.
[6] Gordon, H. L., and Goldman, S., 1989, *Molec. Simul.*, **3**, 213.
[7] Gordon, H. L., and Goldman, S., 1992, *J. phys. Chem.*, **96**, 1921.
[8] Le Bret, M., and Zimm, B. H., 1984, *Biopolymers*, **23**, 271.
[9] Conrad, J., Troll, M., and Zimm, B. H., 1988, *Biopolymers*, **27**, 1711.
[10] Wensel, T. G., Meares, C. F., Vlachy, V., and Matthew, J. B., 1986, *Proc. Natl Acad. Sci. USA*, **83**, 3267.
[11] Murthy, C. S., Bacquet, R. J., and Rossky, J., 1985, *J. phys. Chem.*, **89**, 701.
[12] Nilsson, L. G., Guldbrand, L., and Nordenskiöld, L., 1991, *Molec. Phys.*, **72**, 177.
[13] Gil Montoro, J. C., and Abascal, J. L. F., 1995, *J. chem. Phys.*, **103**, 8273.
[14] Guldbrand, L. E., Forester, T. R., and Lynden-Bell, R. M., 1989, *Molec. Phys.*, **67**, 473.
[15] Bratko, D., and Vlachy, V., 1985, *Chem. Phys. Lett.*, **115**, 294.
[16] Mills, P., Paulsen, M. D., Anderson, C. F., and Record Jr, M. T., 1986, *Chem. Phys. Lett.*, **129**, 155.
[17] Nilsson, L. G., Nordenskiöld, L., and Stilbs, P., 1987, *J. phys. Chem.*, **91**, 6210.
[18] Guldbrand, L. E., 1989, *Molec. Phys.*, **67**, 217.
[19] Gil Montoro, J. C., and Abascal, J. L. F., 1995, *Molec. Simul.*, **14**, 313.
[20] Das, T., Bratko, D., Bhuiyan, L. B., and Outhwaite, C. W., 1995, *J. phys. Chem.*, **99**, 410.
[21] Nishio, T., 1996, *Biophys. Chem.*, **57**, 261.
[22] Torrie, G. M., and Valleau, J. P, 1980, *J. chem. Phys.*, **73**, 5807.
[23] Saenger, W., 1984, *Principles of Nucleic Acid Structure* (New York: Springer Verlag).
[24] Arnott, S., and Hukins, D. W. L., 1972, *Biochem. Biophys. Res. Commun.*, **47**, 1504.
[25] Rossky, P. J., Dudowicz, J. B., Tembe, B. L., and Friedman, H. L., 1980, *J. chem. Phys.*, **73**, 3372.
[26] Vlachy, V., and Haymet, A. D. J., 1986, *J. chem. Phys.*, **84**, 5874.
[27] Abascal, J. L. F., and Turq, P., 1991, *Chem. Phys.*, **153**, 79.
[28] Vorontsov-Velyaminov, P. N., and Lyubartsev, A. P., 1992, *Molec. Simul.*, **9**, 285.
[29] York, D. M., Darden, T., Deerfield II, D., and Pedersen, L. G., 1992, *Int. J. quantum Chem., quantum Biol. Symp.*, **19**, 145.
[30] Bresme, F., and Abascal, J. L. F., 1993, *J. chem. Phys.*, **99**, 9037.
[31] Abascal, J. L. F., Bresme, F., and Turq, P., 1994, *Molec. Phys.*, **81**, 143.
[32] Gil Montoro, J. C., Bresme, F., and Abascal, J. L. F., 1994, *J. chem. Phys.*, **101**, 10892.
[33] Bresme, F., Lomba, E., Weis, J. J., and Abascal, J. L. F., *Phys. Rev.* E, **51**, 289.
[34] Soumpasis, D., 1978, *J. chem. Phys.*, **69**, 3190.
[35] Abramowitz, M., and Stegun, I. A., 1972, *Handbook of Mathematical Functions* (New York: Dover Publications).